Bioconjugate Chemistry

Review

Characterizing Self-Assembled Monolayers on Gold Nanoparticles

Elena Colangelo, Joan Comenge, David Paramelle, Martin Volk, QIUBO CHEN, and Raphael Levy

Just Accepted

ACS Publications

Characterizing Self-Assembled Monolayers on Gold Nanoparticles

Elena Colangelo,[a] Joan Comenge,[a] David Paramelle,[b] Martin Volk,[c,d] Qiubo Chen,[e] Raphaël Lévy[a,*]

[a]Institute of Integrative Biology, University of Liverpool, Crown Street, L69 7ZB Liverpool, United Kingdom

[b]Institute of Materials Research and Engineering, A*STAR (Agency for Science, Technology and Research), 2 Fusionopolis Way, #08-03 Innovis, Singapore 138634

[c]Department of Chemistry, University of Liverpool, Liverpool L69 7ZD, United Kingdom

[d]Surface Science Research Centre, Department of Chemistry, Abercromby Square, University of Liverpool, Liverpool L69 3BX, United Kingdom

[e]Institute of High Performance Computing, A*STAR (Agency for Science, Technology and Research), 1 Fusionopolis Way, #16-16 Connexis North, Singapore 138632

ABSTRACT: A key aspect of nanoscience is to control the assembly of complex materials from a "bottom-up" approach. The self-assembly and self-organization of small ligands at the surface of nanoparticles represent a possible starting route for the preparation of (bio)nanomaterials with precise (bio)physical and (bio)chemical properties. However, surface characterization and elucidation of the structure-properties relationship, essentials to envision such control, remain challenging and are often poorly investigated. This Topical Review aims to discuss different levels of surface characterization, giving an overview of the experimental and computational approaches that are used to provide insights into the self-assembled monolayer with molecular details. The methods and strategies discussed focus on the characterization of self-assembled monolayers at the gold nanoparticle surface, but most of them could also be applied to other types of nanoparticles.

1. Introduction

The Bakerian Lecture given by Michael Faraday in 1857, describing for the first time the interaction of metal particles with light, has been a milestone in the development of the modern science of gold colloids.[1,2] The enticement of gold nanoparticles (GNPs) resides in the way their free electrons interact with light,[3] revealing both their and the environment's properties, together with the ease of synthesis[4,5] and functionalization with small ligands.[6] Thus, small thiolate ligands, including alkanethiols,[7] peptides,[8] oligonucleotides,[9,10] and polyethylene glycols,[11] bind readily to the surface and form self-assembled monolayers (SAMs),[7] imparting both stability[12,13] and desired functionality[14,15] to the nanoparticles. However, even though the literature is abounding with examples of functionalized gold nanoparticles for applications in biology,[16] catalysis[17] and sensing,[18] usually illustrated with inspiring schemes, the actual structure and organization of the SAMs at the gold nanoparticle surface are challenging to assess and remain often poorly characterized. Such elucidation is a fundamental prerequisite to warrant data reproducibility and build knowledge of predictable properties on the basis of the nanomaterials' characteristics. Moreover, the investigation of the relationship between structure and function is necessary to fully exploit the possibility of engineering nano-objects with well-defined (bio)physicochemical and structural properties from a "bottom-up" approach, which could then be assembled into complex networks, potentially taking inspiration from nature.[19,20]

Starting from basic properties, such as overall chemical composition and thickness, and progressing to more advanced insights, such as molecular structure and phase separation of ligands, we review the current knowledge and the methods available to characterize these systems.

As the Topical Review is organized according to self-assembled monolayer properties, the same studies may appear in different sections. Overall, this Topical Review aims to highlight the web of connections existing between the different self-assembled monolayer characteristics.
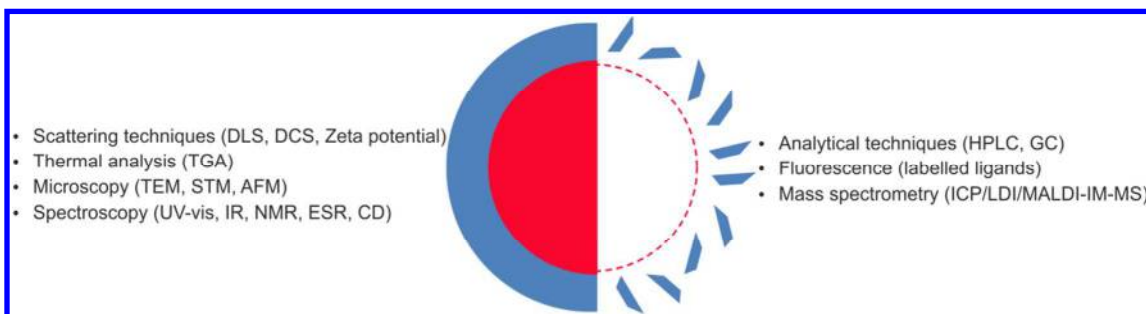
2. Basic Characterization and Composition

As mentioned in the introduction and also highlighted in previous reviews,[7,21] many scientific articles lack basic characterization of functionalized GNPs. Thus, in this section, some of the chemical and analytical approaches and techniques adopted to characterize a SAM on GNPs and shed light on its composition are recapitulated.

Once the GNPs are synthesized, the stabilizing molecules at the surface, e.g., citrate ions[4] or simple thiols,[5] can be replaced by another thiol-containing molecule in a ligand exchange reaction, following an associative reaction with 1:1 stoichiometry.[22] The stabilizing molecules ensure colloidal dispersion of the GNPs, typically by electrostatic and/or steric repulsion.

Scheme 1 lists the most common experimental methods used to characterize the ligands bound to the nanoparticle surface, which will be discussed throughout this Topical Review. Such methods can be divided into those that analyze directly the ligand-capped GNPs and those that require the release of the ligands (Scheme 1).

The first category includes UV-visible spectrophotometry. Indeed, GNPs larger than 2 nm in diameter are characterized by the surface plasmon band (SPB),[23] theoretically described by Mie in his work dating from 1908;[24] the position of the SPB maximum is deeply influenced by the GNP size and shape and the dielectric constant of the surrounding environment. Hence, the presence of ligands anchored onto the surface can be indirectly probed by a shift in the SPB maximum detected simply by UV-vis spectrophotometry.

- Scattering techniques (DLS, DCS, Zeta potential)
- Thermal analysis (TGA)
- Microscopy (TEM, STM, AFM)
- Spectroscopy (UV-vis, IR, NMR, ESR, CD)

- Analytical techniques (HPLC, GC)
- Fluorescence (labelled ligands)
- Mass spectrometry (ICP/LDI/MALDI-IM-MS)

Scheme 1. Examples of experimental methods used to characterize the GNP's surface, analyzing ligand-capped GNPs (left) or ligands released upon gold decomposition or ligand exchange (right).

Also, indirect evidence of functionalization can be obtained from the increased colloidal stability in high ionic strength media that otherwise would lead to complete particle-to-particle aggregation, i.e., red-shift and broadening of the SPB.[25] Weisbecker et al., for instance, investigated the effect of capping citrate GNPs with alkanethiols of different chain lengths and terminal functional groups in various conditions of pH and ionic strength by monitoring the absorbance spectra over time;[26] Lévy et al. observed a 2 nm red-shift and protection to salt-induced aggregation

resulting from the conjugation of the CALNN pentapeptide to citrate GNPs (Figure 1A).[8] Duchesne et al. observed different GNP stability against electrolyte-induced aggregation and ligand exchange upon varying the ligand concentration during the conjugation process, thus providing an indirect measurement of the ligand capping density on GNPs.[12] Evaluation of the resistance of capped GNPs to increasing concentrations of dithiotreitol, i.e., ligand exchange, was used to select combinations of ligands forming highly compact SAMs on GNPs, hence providing high stability in biological environments.[13] Similarly, indirect estimation of the SAMs' compactness was gathered by Schulz et al. from assessing the resistance to cyanide etching of GNPs capped with SAMs constituted of PEG-thiol ligands with the same chain length, but with the segments between the thiol group and the polymer moiety of different sizes and chemical functionalities (Figure 1B).[27]

Furthermore, differential centrifugal sedimentation[28] (DCS) or dynamic light scattering (DLS) and zeta (ζ) potential measurements[29] are used to determine the hydrodynamic diameter and the charge of the ligand-capped GNPs, respectively, thus giving insight into their stability and properties, such as protein[30] or molecule[31] adsorption. Thermal gravimetric analysis (TGA), by monitoring changes in weight over a temperature ramp, gives an indication of the amount of ligands on the GNPs, but requires 1-10 mg of sample and assumptions and modelling for the shape of the gold cores.[32] IR and NMR spectroscopies are generally used not only to characterize the content of SAMs on GNPs, but also to investigate their structure and interactions existing between the ligands; thus, they will be further discussed in Section 4.

Examples of analytical methods to identify and quantify the amount of ligands upon cleavage from the GNPs surface include Zhou et al.'s work where SAMs constituted of up to three different ligands were first cleaved from the NP surface with I_2,[33] then identified by mass spectrometry and quantified by high-performance liquid chromatography with UV or chemiluminescent nitrogen detection (HPLC/MS/UV/CLND), using calibration curves constructed from the free ligands.[34] This provided a method to confirm the common assumption that the ratio of ligands on the GNP surface is the same as the one used during the conjugation process (Figure 1C). However, as Fisher et al. pointed out, this method is limited to disulfide ligands and cannot quantitatively analyze mixtures of simple alkanethiol ligands because of disulfide formation upon I_2 exposure.[35] Thus, Fisher et al. developed a method to quantify the amount of alkanethiol ligands in mixed SAMs on 2 nm GNPs using gas chromatography coupled to mass spectrometry (GC/MS/MS), upon I_2 exposure, and using a calibration curve constructed from free disulphide mixtures; ^{1}H-NMR spectroscopy was employed as an additional technique to corroborate their findings.[35] Hinterwirth et al.[36] described a method to determine the ligand capping density on the basis of the observed linear relationship between the NP diameter, measured by transmission electron microscopy (TEM), and the ratio between gold and sulfur atoms, measured by inductively coupled plasma mass spectrometry (ICP-MS), a powerful technique for elemental analysis.[37] The number of peptide ligands can also be measured using amino acid analysis.[8,12]

To quantify the amount of alkanethiol-oligonucleotides capping a GNP, Demers et al. modified the ligand by fluorescently labelling it, and then, after conjugation to the GNPs and removal of the ligand excess, incubated the capped GNPs in the presence of another thiolate ligand. Thus, the fluorescently labelled oligonucleotides were released by ligand exchange and quantified using fluorescence, based on calibration curves made from the free fluorescently-labelled ligand in solutions of same pH and ionic strength (Figure 1E).[38] The ligand exchange reaction was
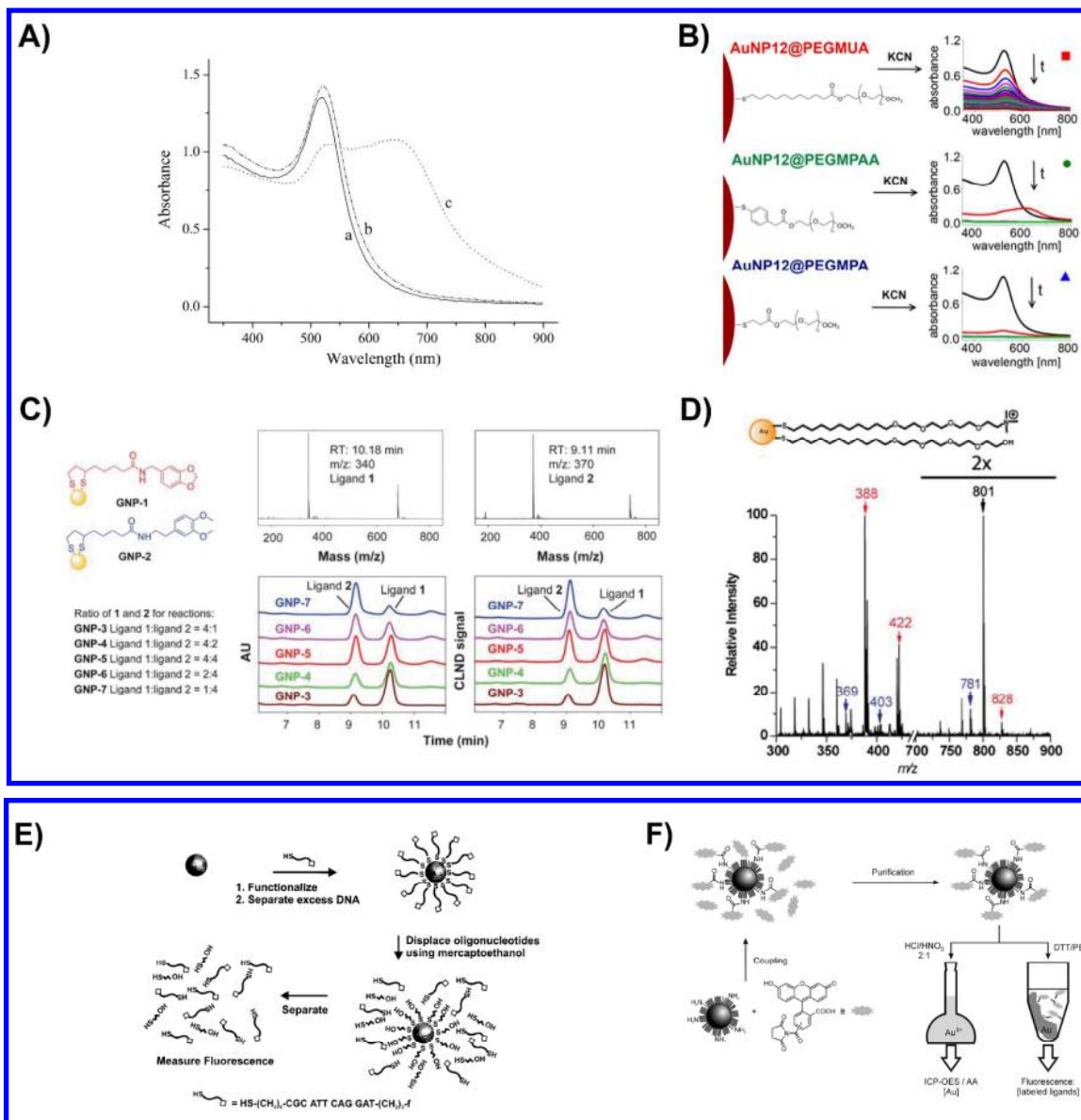
Figure 1. Measurements of the presence and composition of SAMs on GNPs; using GNP optical properties: A) UV-vis spectra of citrate GNPs before (a) and after addition of a volume of CALNN peptide (b) or phosphate-buffered saline (c) (Reprinted from ref. 8), B) Schematic drawings and UV-vis spectra recorded in 5- (top) or 2- (middle-bottom) min steps of differently capped 12 nm GNPs before (black lines) and after addition of KCN (Reprinted from ref. 27); using mass spectrometry techniques: C) Mass spectra of the thioctic acid ligands (shown on the left) cleaved from the GNPs and quantified by HPLC using two detectors (adapted from ref. 34), D) LDI-MS spectra of a mixed SAM on GNPs showing ions corresponding to both ligands (in blue and red) and mixed disulphide ions (in black) (Adapted from ref. 39); using fluorescence: E) GNPs functionalized with a fluorescent-ly labelled ligand and purified from its excess. Upon ligand exchange and release of the ligand, the fluorescence is measured and the ligand quantified (Reprinted from ref. 38), F) Upon fluorescence labelling of a reactive group and removal of the fluorophore excess, the GNP concentration is determined by ICP upon dissolution in aqua regia, and the fluorescence corresponding to the amount of reactive group is measured upon ligand exchange (Reprinted from ref. 40).

confirmed to be completed by an independent method, where the GNPs were dissolved by cyanide and the increase in fluorescence, associated with the fluorophore being released, monitored. Maus et al. used a similar method to quantify something conceptually different, i.e., the average amount of functionalizable reactive groups per GNP,

4

where the GNPs were capped with a mixed SAM constituted of a ω-carboxylate and ω-amino thiols; the last one functionalizable with a fluorescently labelled NHS ester derivative (Figure 1F).[40]

Functionalized GNPs can also be characterized by laser desorption ionization mass spectrometry (LDI-MS).[41–43] The use of this technique for characterizing nanoparticles originates from Tanaka et al.'s work,[44] demonstrating the ability of metal nanoparticles to absorb laser light energy and thus desorb analytes and enhance their ionization. For instance, Yan et al. characterized GNPs capped with positively or negatively charged and neutral ligands by LDI-MS: in all cases, both thiol and disulphide ions were detected.[39] Moreover, when analyzing GNPs functionalized with two different ligands, not only thiol and disulphide ions corresponding to both ligands were identified, but also mixed disulphide ions (Figure 1D). The authors developed a procedure to provide a semi-quantitative measurement of two ligands on GNPs; since different ionization efficiencies are associated to different ligands, NMR spectroscopy was used as external technique for calibration.

Cliffel and McLean's group developed a strategy coupling MALDI to ion mobility-mass spectrometry (IM-MS), a gas-phase separation technique, to provide a measurement of the relative quantities of two ligands in a mixed SAM on GNPs.[45] This technique is more advantageous than NMR spectroscopy, since it does not require the two ligands to have different functionalities. Also, unlike traditional MS, IM is able to separate ions corresponding to clusters of gold atoms and ligands from those corresponding to ligands alone, thus proving that the ligands were actually attached to the GNP surface.

3. Compactness and Thickness

As discussed in the previous section, different approaches have been proposed in the literature to determine the amount of ligands on GNPs, hence the capping density. Whilst not independent of the capping density, the SAM compactness and thickness also depends on the conformation of the ligands and on the amount of solvent present within the SAM. In this section, direct and indirect methods providing insights into these characteristics are detailed.

The compactness of a SAM does not only result from the number of ligands on the GNPs surface; Chen et al. have indeed reported the extremely high stability against ligand exchange of SAMs constituted of peptidols with aromatic amino acids, i.e., H-CFFFY-ol or H-CFFFT-ol, and PEGylated alkanethiol, indicating that aromatic and alkyl chains can form extremely compact SAMs through hydrophobic interactions and, possibly, well-defined secondary structure motifs.[13] Duchesne et al. highlighted that higher SAM compactness can be achieved by using modified peptides, i.e., peptidols, which bear a non-ionisable primary alcohol group, instead of a carboxyl group, at the C-terminus.[12] Schulz et al., as previously mentioned, probed the effect which segments of different sizes and chemical functionalities between the thiol group and a polymer chain had on protecting the GNPs from cyanide etching, thus showing the effect of the segments on the capping density, hence compactness and stability to etching (Figure 1B).[27]

The packing of a SAM can be measured more directly *via* its thickness, which, however, can be challenging to assess. Since GNPs are electron dense materials, they have been used for over 60 years as contrast agents in transmission electron microscopy (TEM).[46] Even though TEM is mostly used to size the gold cores only, Jürgens et al.

measured the thickness of films of proteins adsorbed on GNPs with this technique.[47] Ardao et al. imaged by TEM samples of enzyme-adsorbed GNPs, not purified from the excess of enzyme, using the negative staining method.[48] The agent, by staining the enzymes' surface, conferred a grey background to the images. Since the enzymes at the GNPs' surface were highly packed and thus did not get stained, the ligand shells appeared as white rings in the TEM images. However, considering the drying of the sample and the often insufficient contrast, TEM images cannot provide quantitative information on the thickness of SAMs in solution.

As mentioned in Section 2, dynamic light scattering (DLS) is a common method to determine the hydrodynamic diameter of GNPs,[29] but it requires rigorous experimental conditions in order to avoid data misinterpretation.[49] Its value depends on the length of the ligands and the compactness of the monolayer. Therefore, changes of these parameters can be reflected by DLS measurements. However, small changes in the hydrodynamic diameter (<5%) cannot be detected by DLS. Walkey et al., for instance, assessed by DLS the hydrodynamic volume occupied by one poly(ethylene glycol) (PEG) molecule in SAMs of different capping densities on GNPs of different sizes.[50] Smaller volumes were found for higher capping densities, indicating both strengthening and dehydration of the ligands. On the other hand, for a given capping density, a larger volume was found for smaller GNPs, which was rationalized with the fact that a decrease in GNP size, i.e., an increase of curvature, frustrates the hydrophobic interactions between the PEG chains (Figure 2A). Belsey et al. described two approaches to measure the thickness and derive the number of either adsorbed proteins or conjugated peptides on GNPs of different sizes.[51] The first approach involved UV-Vis spectroscopy to indirectly prove the adsorption/conjugation of the biomolecules to the GNPs, by monitoring the surface plasmon band, DLS to measure the thickness of the monolayers, and differential centrifugal sedimentation (DCS) to prove the monodispersity of the GNPs. The second approach employed X-ray photoelectron spectroscopy (XPS) to measure the monolayer thickness in ultrahigh vacuum. The authors concluded that in spite of the intrinsic differences between the two approaches, the results appeared to be consistent. Also, Torelli et al. developed a computational model for determining the ligands' capping density from XPS data for poly(ethylene glycol) alkanethiol-capped GNPs of different sizes.[52]

Falabella et al.[53] and Krpetić et al.[28] highlighted the advantages of using analytical ultracentrifugation (AUC) techniques, determining the GNPs' sedimentation coefficients, as compared to DLS. In particular, contrarily to DLS, AUC measurements are not perturbed by the presence of small GNPs aggregates, which, in the case of DLS, would potentially dominate the analysis. Falabella et al. characterized GNPs of different sizes, functionalized with thiol-terminated single stranded DNA, to investigate the effect of capping density and chain length;[53] Krpetić et al. measured the shell thickness of a range of PEG-thiol and peptide ligands on GNPs of different sizes (Figure 2B).[28]
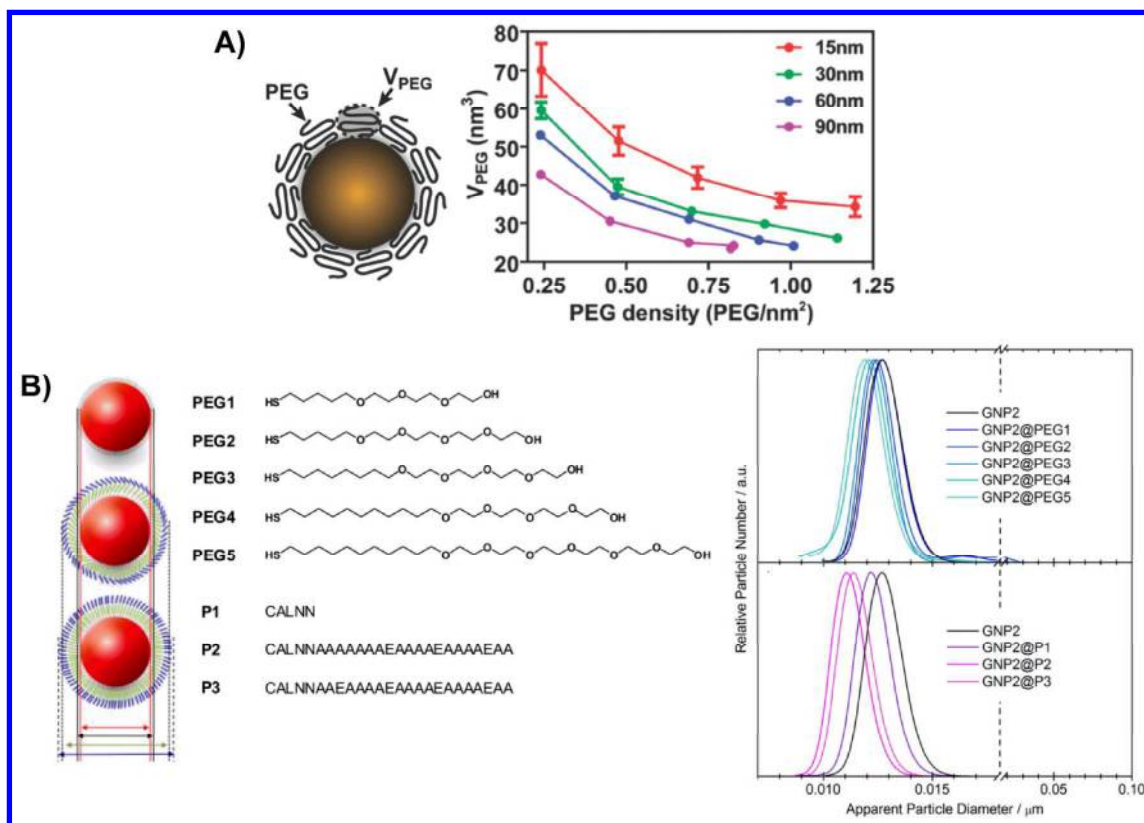
Figure 2. Compactness and thickness of SAMs on GNPs. A) Schematic representation and PEG chain hydrodynamic volume (V_{PEG}) determined by dynamic light scattering (DLS) as a function of PEG capping density on GNPs of different sizes (Adapted from ref. 50); B) Normalized number size distributions of the GNPs illustrated on the left and capped with different ligands. Analysis by differential centrifugal sedimentation (DCS) shows a shift to smaller apparent diameter with the increase in ligand shell thickness, which can be corrected, so that the actual shell thickness is obtained (Adapted from ref. 28).
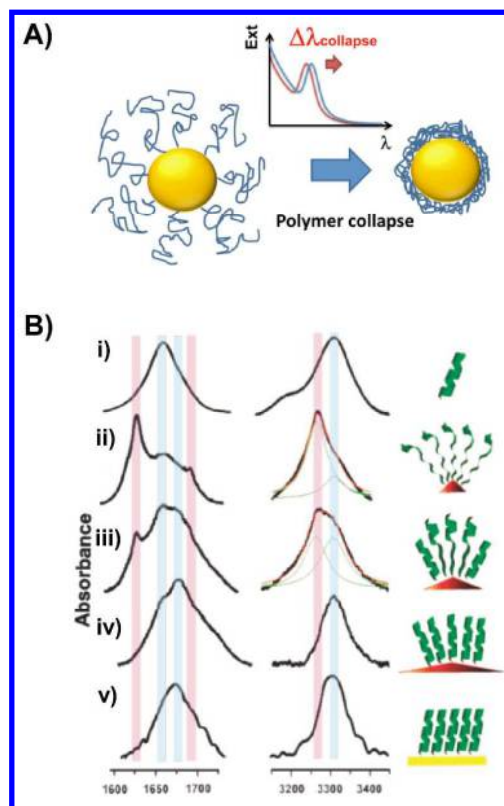
4. Conformation

As discussed in the previous section, measurement of the SAMs' thickness and compactness also provides insights into the underlying ligands' conformation. However, determining the structure of ligand-capped GNPs at the molecular level remains highly challenging.

The work by Jadzinsky et al., dating from 2007, marked a breakthrough in terms of structural information on GNPs.[54] The authors determined the crystal structure at 1.1 Å resolution of *p*-mercaptobenzoic acid-capped 1.5 nm gold clusters and thus, shed light on the structure and geometry of a thiol monolayer. Azubel et al., in their work dating from 2014, solved the structure at atomic resolution of a smaller thiol-capped gold cluster by aberration-corrected transmission electron microscopy.[55] In the years in between these two works, capped GNPs in the 1-3 nm range were crystallized, but X-ray diffraction structures with high resolution were not obtained.

Therefore, even though the structures of gold clusters that have been effectively solved provide precious information, other approaches have to be sought to elucidate the conformation of ligands on GNPs larger than 2 nm. Examples of such attempts are described in this section.

Comenge et al. functionalized ~15 nm GNPs with different ratios of 11-mercaptoundecanoic acid (MUA) and thiolated PEG (MW 3.4 KDa) to modulate the biological responses that SAMs of either PEG or alkanethiols on GNPs trigger.[56] Using a combination of UV-vis and DLS techniques, the authors found that the changes in GNP properties were correlated with different PEG conformations. The hydrodynamic radius of the functionalized GNPs was found to suddenly increase at a ratio between PEG and MUA of ~0.7, marking the straightening of the PEG ligands into a brush-like conformation. The blue-shift of the surface plasmon band (SPB) maximum at this ratio corroborated the change in PEG conformation. On this note, Tagliazucchi et al. presented a theoretical method to calculate the optical properties of GNPs capped with SAMs of different conformations, which have different densities and hence refractive indices, and thus were able to correlate the position of the SPB with a change in conformation.[57] The theoretical results were found to well describe the optical properties of GNPs functionalized with a thermoresponsive polymeric monolayer (Figure 3A), i.e., the red-shift of the SPB upon polymer collapse, as well as the effect of capping density, chain length and GNP size on the extent of the shift. Xia et al. characterized by DLS gold nanocages with side lengths of 30, 50 and 60 nm, functionalized with PEGs of different molecular weights.[58] The largest hydrodynamic diameter corresponded to the GNPs capped with the PEG molecules of intermediate size. Hence, it was concluded that the SAM constituted of the largest PEGs assumed a mushroom-like conformation, i.e., chains back-folding on the GNPs.

Figure 3. Conformation of SAMs on GNPs. A) Schematic representation of the surface plasmon band red-shift upon collapse of a thermoresponsive polymeric monolayer on GNPs (Reprinted from ref. 57); B) FTIR bands of a Leu-rich peptide (i) free in solution; (ii-iv) Leu-peptide-capped GNPs (5, 10, 20 nm diameter, respectively) and (v) on a planar gold surface. Blue and pink stripes are indicative of α-helix and β-sheet conformations, respectively (Adapted from ref. 59).

Spectroscopic techniques, such as IR and NMR, were cited in Section 2 as means to characterize the composition of SAMs on GNPs. However, these techniques provide information not only about the functionalization and the average ratio of ligands at the GNPs surface, but also about the structure of the ligands within the SAM and the intermolecular interactions existing between them.

Murray and co-workers characterized by FTIR GNPs from 1.5 to 5.2 nm in diameter capped with dodecanethiolate ligand.[32] The IR spectra were taken in solid-phase and allowed the investigation of the alkyl chain conformation. More ordered SAMs, corresponding to a *trans* zigzag structure, similar to the structure observed on planar gold surfaces, were found on the larger GNPs. However, considering the relatively small size of the largest GNPs and that ordered monolayers were already distinguished on 4.4 nm GNPs, the authors investigated the role of sample preparation in such observations. Therefore, the structure of alkanethiols of different chain lengths on ~2 nm GNPs was analyzed by FTIR both in solid-phase and in solution.[33] It was found that shorter alkanethiols adopted a highly ordered conformation on these 2 nm GNPs in solid-phase, but became quite disordered in carbon tetrachloride, highlighting the importance of the sample preparation, as it can lead to changes in the ligands conformation. Moreover, Murray and co-workers listed the factors determining the broadening of thiolate-capped GNP ^{13}C and ^{1}H NMR spectra.[32,60] Importantly, since both the ligands' proximity to the gold surface and the density of packing contribute to spectral broadening, NMR analysis provides information about the ligands' environment and structural features. The spectra, however, can be difficult to interpret.

Peptide-capped GNPs have been described by us as building-blocks that could potentially be engineered into advanced nanoparticles with protein-like properties.[19] Hence, determining their structures is of crucial importance.

Fabris et al., prepared GNPs of ~1-2 nm size, capped with peptides made of α-aminoisobutyric acid residues.[61] Homooligomers of this residue (starting from the tripeptide) are known to form stiff secondary structure motifs, i.e., β-turns and 3_{10}-helices. IR analysis indicated the presence of 3_{10}-helices, stabilized by intra-peptides hydrogen bonds, both in solution and at the surface of GNPs, independently of the peptide length. Also, the authors judged inter-peptide hydrogen bonds, identified by NMR analysis, to underlie the rigid conformation observed in all the systems investigated. Thus, building-blocks characterized by a stiff monolayer and a precise secondary structure motif were provided. It is worth noting that the IR spectra of the capped GNPs, taken both in solid-phase and in solution, did not show any significant difference.

Shaw et al. investigated the effect of GNP size, i.e., curvature, on the secondary structure of CALNN and CFGAILSS peptide SAMs.[62] The authors used GNPs of 5, 10 and 25 nm in diameter, and a combination of FTIR and solid-state NMR (ssNMR) to elucidate these structures. The CALNN peptide was found to adopt a random coil conformation independent of the GNP size. The CFGAILSS peptide, which arranged in amyloid fibers with an antiparallel β-sheet conformation in solution, formed parallel β-sheets when attached to the gold surface, which were more pronounced on the largest GNPs. Hence, the number of adjacent peptides forming inter-peptide hydrogen bonds and thus, parallel β-sheets, is dictated by the nanoparticle curvature, which agrees well with a simple geometrical model. Moreover, ssNMR directly demonstrated the presence of inter-peptide hydrogen bonds only in the case of CFGAILSS and excluded the interdigitation between GNPs. Similarly, Mandal et al. capped GNPs of 5, 10 and 20 nm in diameter, with a Leu-rich peptide.[59] FTIR analysis in solid-phase demonstrated the presence of a greater

content of α-helix motif on the GNPs with a lower curvature, similar to the one observed for the free peptide or on a planar gold surface, whereas GNPs with high curvature were dominated by β-sheet structures (Figure 3B). The authors suggested that this was due to high capping densities at the edges and corners of GNPs, caused by the high unsaturation of the gold atoms. High capping densities, in turn, allow for the efficient formation of inter-peptide hydrogen bonds which are the prerequisite for forming β-sheet structures. Since in small GNPs, edges and corners dominate over planar faces, more β-sheet structures were found for these, whereas in 20 nm GNPs, binding to planar faces seemed to be predominant, leading to the native α-helical peptide structure. Thus, both works highlighted the importance of GNPs size and ligand sequence when designing nanomaterials with well-defined secondary structure motifs.

On a different note, Rio-Echevarria et al. confirmed by circular dichroism (CD) that the helical secondary structure of an undecapeptide was maintained after conjugation to GNPs of 1-2 nm.[63] However, measuring the CD of larger GNPs in the UV region (to elucidate the conformation of the peptide SAM) can be problematic due to the high absorbance of the gold cores.

5. Organization of Mixed Self-Assembled Monolayers

Since the ratio of ligands at the GNPs surface does not necessarily reflect the one used during conjugation, in Section 2 we summarized some of the efforts made to quantify the ligands constituting a mixed SAM on GNPs. However, questions related to the organization of mixed SAMs on GNPs should also be addressed.

In the 90s, studies of wetting, performed with ellipsometric and goniometric measurements, suggested that two alkanethiols of different chain length and with either a methyl or hydroxymethyl terminal functional group phase-separate on a planar gold surface, forming microscopic islands (Figure 4A).[64] Topological characterization with scanning tunneling microscopy (STM) by Stranick et al.[65] confirmed such phase separation into domains, whose shapes were found to be time-dependent, for two alkanethiols of the same length, but having different non-interacting terminal groups, i.e., methyl and methyl ester, on a gold surface. Tamada et al.[66] studied the segregation of mixtures of alkanethiols with different chain length at different ratios on gold with atomic force microscope (AFM) and observed clear phase separation.
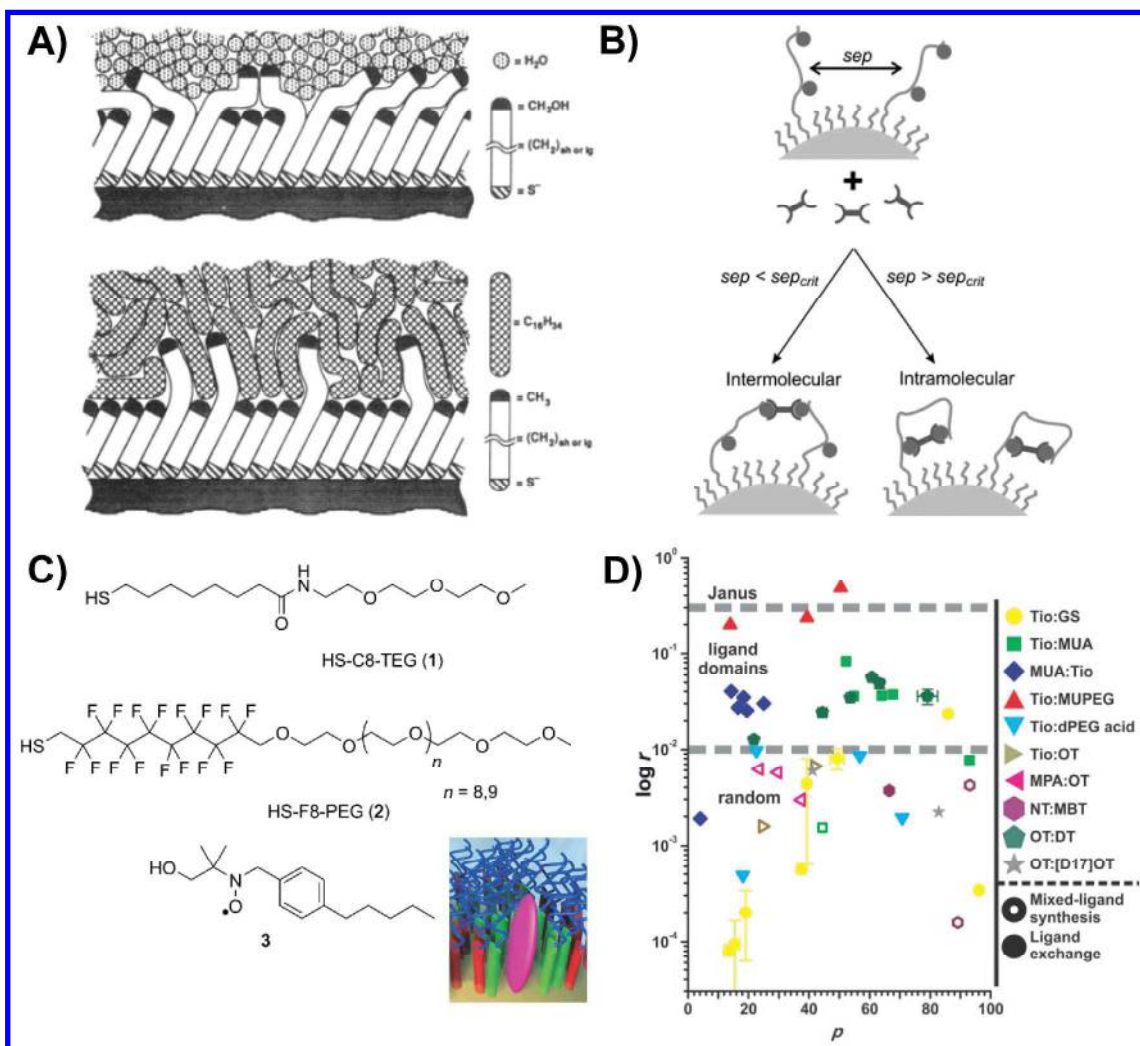
10

Figure 4. Organization of mixed SAMs. A) Schematized wettability on a planar gold surface of a mixed SAM of alkanethiols of different lengths with an hydroxymethyl or methyl terminal group in water (top) or hexadecane (bottom), respectively (Reprinted from ref. 64); B) Schematized proximity probes in a CALNN monolayer on GNPs forming, depending on their separation, either an inter- or intramolecular cross-link (Reprinted from ref. 67); C) Chemical and conceptualized structures of the ligands constituting the mixed SAM (1,2; red, green) and radical probe (3; magenta) (Adapted from ref. 68); D) Residual sums of squares versus different ratios of ligands for different mixed SAMs on GNPs, prepared following two different procedures, and characterized by MALDI-IM-MS, depicting different types and extents of ligands segregation (Reprinted from ref. 69).

In 2004 Jackson et al.[70] reported the first work on GNPs presenting a stripe-like arrangement of ligands. The authors claimed that STM images of GNPs capped by a mixture of an alkanethiol and a longer thiolate molecule with a terminal carboxylic acid group demonstrated the presence of ordered domains of 5 Å in size within such SAMs. Moreover, such domains were described as parallel stripe-like patterns circling around the gold cores with shape and size tunable by selecting the composition of the ligand mixture and the GNP size, and with quite alluring properties arising from their small dimensions, such as avoiding the non-specific adsorption of proteins. However, this body of work has been subject of controversy and the published results, re-examined by Cesbron et al.[71] and Stirling et al.,[72] have been suggested to be the result of instrumental artefacts and erroneous analyses. Both of these

11

analyses received a response from the authors of the original publication that addressed the arguments of invalidation of the results obtained.[73,74]

Other approaches to assess the organization of mixed SAMs include Duchesne et al.'s work where GNPs were capped with CALNN and a functional peptide, containing two reactive groups, and acting as a proximity probe.[67] Intermolecular cross-linking between two functional peptides was expected if their separation was lower than 4 nm; if greater, intramolecular cross-linking should have been detected (Figure 4B). Using this method, the authors showed that even if there were only two or three functional peptides on a GNP, they had the tendency to be close to each other on the GNP surface; i.e., they organized in a small domain. This packing was found to form during the self-assembly of the mixed monolayer, and not when the functional peptides were still free in solution. Prins' group used a range of probes to assess the organization of mixed SAMs.[75,76] In a first approach, the SAMs were constituted of different ratios of thiolate ligands with either a cationic or neutral terminal group, where the positively charged group was able to catalyse the transphosphorylation of a substrate, and the apparent catalytic rate constant k_{cat} was used to probe the SAMs' organization.[75] The GNPs' catalytic activity was found to gradually increase up to ligand ratios of ~0.4 and then to remain constant; this increase was ascribed to a random distribution of the ligands within the SAMs. In ref. [76], the same authors discussed the disavantages of k_{cat} as parameter and proposed a general methodology to assess the morphology of a mixed SAM, without the need of a catalytic ligand. A fluorescent anionic probe was used, whose fluorescence is quenched upon interaction with the GNP surface, thus allowing for easy determination of its binding to the cationic ligands, the extent of which depends on the ligands' organization on the GNP surface. A random distribution of the ligands up to ratios of ~0.4 was concluded from both methodologies and was supported by simulated saturation profiles. Gentilini et al. observed a different surface organization and ordering in mixed SAM on GNPs they investigated. They used a radical probe to assess the organization of mixed SAMs constituted of perfluoroalkyl and alkyl amphiphilic thiolate ligands (Figure 4C) on GNPs by electron spin resonance (ESR) spectroscopy.[68] The radical probe was able to sense the hydrophobicity of the environment and was characterized by different hyperfine splitting constants when sensing a SAM constituted of either perfluoroalkyl or alkyl thiolate ligands. Thus, the authors showed that, up to a ratio of 2.5 between alkyl and perfluoroalkyl ligands, the probe sensed a fluorinated environment, indicating the packing within islands of such ligands.

Cliffel and McLean's group used MALDI coupled to ion mobility-mass spectrometry (IM-MS) to investigate the phase segregation of two ligands in a mixed SAM on GNPs.[69] Upon MALDI analysis, gold-thiolate ions were generated and, once separated from the ligands' ions by IM-MS, the information regarding a particular type of gold-thiolate clusters, i.e., Au_4L_4, was extracted and quantitatively compared to a theoretical model based on the binomial distribution. Using this method, the authors, characterizing several mixed SAMs of different compositions and ratios, observed various degrees of ligands segregation (Figure 4D).

Additionally, from the analysis of the cross peaks in two dimensional NMR nuclear Overhauser effect spectroscopy (NOESY) spectra, information on the nucleis' proximity can be obtained. Thus, Kohlmann et al. showed that NOESY can reveal the packing of SAMs of both tiopronin and alkanethiol ligands on gold nanoparticles of different sizes.[77] Also, Pradhan et al. used NOESY NMR to demonstrate ligand segregation within mixed SAMs on 2 nm GNPs following sample preparation under conditions known for forming either phase-separated or homogene-

ously mixed SAMs.[78] Similarly, Liu et al. used a combination of one and two dimensional NMR to elucidate the organization of aliphatic and aromatic thiols at different ratios on GNPs.[79]

Finally, efforts made to impart different chemical functionalities or polarity to the two hemispheres of an organic or inorganic core are worth mentioning. Such category of micro- and nanoparticles was described for the first time with the term "Janus" by De Gennes in 1991.[80] We refer the reader to past reviews highlighting the various procedures investigated to insert elements of dissymmetry within the monolayer.[81,82] The most common method involves an anisotropic environment, e.g., the interface between air/water or immiscible liquids, that drives the self-organization of a SAM constituted of hydrophilic and hydrophobic ligands.[83,84]

6. Modelling

We refer the reader to a recent review recapitulating the different computational methods available to gather a better description and understanding of the interactions between a gold surface or nanoparticle and the surrounding biological environment.[85] In particular, here we consider the limited insights into the SAM's structure and organization that can be obtained with experimental techniques, and the information about SAMs on GNPs that can be obtained with molecular details using a combination of experimental and computational approaches.

Considering that alkanethiol-capped GNPs have been investigated since the early '90s, it is not surprising that several classical force fields (FF), describing the interactions of alkanethiols on gold, are reported in the literature.[86–89] Glotzer and co-workers reported for the first time an atomistic molecular dynamics (MD) study investigating the structure of alkanethiols on gold nanoparticles as a function of temperature, length of the ligand and GNP size; the sulfur atoms were fixed at a distance of 0.238 nm from the gold surface.[90] Ligands with 13 carbons on a 7 nm GNP did not exhibit long-range order at high temperatures, i.e., 900 and 600 K, while they did group into bundles with the same angle to the surface normal at low temperatures, i.e., 450 and 300 K. At 300 K, long-range order was reported only for alkane thiols with more than nine carbons. At high temperatures, the monolayer constituted of the ligands with 13 carbons was found to be more ordered on the larger GNPs, as illustrated by a decrease in the smallest average distance between adjacent terminal groups with an increase in GNP size.

Moreover, Glotzer and co-workers[91] performed atomistic molecular dynamics and mesoscale dissipative particle dynamics simulations to investigate the origin of the stripe-like patterns observed by Jackson et al.[70] They modelled the GNP surface as a sphere and simulated the GNPs capped with an equimolar mixture of immiscible alkanethiols, varying the length and the functional terminal group of the ligands, and the GNP size. According to the authors, a sufficient gain in conformational entropy was needed for the formation and stabilization of the stripe-like patterns. The entropy gain, due to the additional ligand-ligand interfaces in comparison to a bulk-separated system like the Janus one, was found to be dependent on the difference in length between the ligands, on the terminal functional groups, and on the GNP curvature. Furthermore, the authors argued that in case of sufficient entropy gain, the stripe-like patterns were corresponding to the morphology at the equilibrium. For instance, while stripe-like patterns were found on GNPs capped with a mixture of ligands with well-defined length ratios or with different terminal functional groups, a Janus organization was observed on small GNPs or in SAMs constituted of two short alkanethi-

ols with small terminal functional groups and similar length. In a subsequent work, Glotzer and co-workers used atomistic molecular dynamics simulations to study the factors influencing the thickness of the stripe-like motifs.[92]

Velachi et al.[93] and Van Lehn et al.[94] performed atomistic MD simulations at room temperature and in explicit solvent to investigate the relationship between the arrangement of alkanethiols and the hydration properties of mixed SAMs constituted of equimolar alkanethiols of different lengths with either a hydrophilic or hydrophobic terminal functional group on GNPs of different sizes. The sulfur atoms were fixed on the gold surface and three pre-defined types of surface morphology were considered, namely, random, stripe-like (or patchy) and Janus arrangements.

However, Fetisov et al. argued that the simulation methods adopted by Glotzer and co-workers[91,92] were not suitable to explain the formation of stripe-like patterns on GNPs, and that the structures analyzed by Velachi et al.[93] and Van Lehn et al.[94] were not representative of the thermal global equilibrium.[95] Thus, in order to study the phase separation and the resulting surface morphology of mixed SAMs on GNPs and analyze the thermodynamically equilibrated structures, Fetisov et al. used Monte Carlo simulations to investigate the organization of mixed SAMs constituted of equimolar alkanethiols of different chain length, but same terminal functional group, on GNPs of different sizes. The ligands were anchored on the gold surface through their sulfur atom and initially placed in either a random or Janus arrangement. After equilibration, SAMs constituted of ligands differing in length by four methylene groups did show some degree of phase segregation at room temperature, whereas SAMs constituted of alkanethiols with 6 and 14 carbons did present a Janus arrangement. In contrast to Glotzer and co-workers[91,92] studies, the stripe-like organization was only transiently observed during the formation of the Janus arrangement. Also, Gkeka et al. used a coarse-grained model for GNPs capped with hydrophilic and hydrophobic ligands.[96] The authors found by coarse-grained molecular dynamics that even when a stripe-like arrangement of the coarse-grained beads was imparted to the initial structure, the hydrophilic and hydrophobic areas tended to reorganize into homogeneous patterns.

Modelling strategies can help elucidating the structure of peptide-capped GNPs and contribute toward the design of new bio-nanomaterials and complex nanosystems. Despite the large number of publications regarding peptide-capped GNPs, not many MD computational studies investigating the SAM structure at the gold surface are reported in the literature. However, it is worth mentioning that the first classical FF, specifically designed for biomolecules on Au(111) surface, dates only from 2008.[97] In this FF and in its implemented version,[98] both the secondary interactions between the amino acids and the gold surface and the gold polarization induced by the biomolecules and surrounding solvent molecules are taken into account.

Simulated peptide-capped GNPs using simpler approximations include Duchesne et al.'s work, where MD simulations were used to assess the volume accessed by a functional peptide embedded in a CALNN monolayer, which was represented by only the C-terminal residues, reproducing a surface with a curvature appropriate for a CALNN layer on a 10 nm GNP.[67] Todorova et al. investigated the effect of TAT concentration, i.e., a cell-penetrating peptide, on the structure and compactness of a CALNN monolayer anchored through the cysteine sulfur atoms on a 3 nm GNP built from neutral carbon-type atoms.[99] The computational results indicated higher effective diameter of the capped GNP and higher water exposure of the TAT basic residues on GNPs capped with an intermediate TAT concentration. The authors tested the cell internalization of the differently capped GNPs and claimed that

14

TEM images and inductively coupled plasma-atomic emission spectroscopy (ICP-AES) provided evidence of higher internalization in the case of GNPs capped with an intermediate concentration of TAT, thus validating the properties foreseen by the computational model. A direct validation of the computational findings in terms of the hydrodynamic radius was prevented by the small size of the GNPs, though. Lee et al. looked at the effect that conjugating single peptides of different sequences to 5 nm GNPs had on their structure and dynamics, in comparison to when free in solution.[100] Colangelo et al. recently presented a MD computational model for peptide-capped GNPs, which was validated by the good agreement with experimental results, and showed the dependence of the peptide secondary structure on GNP size and peptide capping density.[101] Moreover, the model provided detailed insights into the SAMs' structural and dynamic properties, such as the peptides' organization into secondary structure domains, which could not have been assessed experimentally. Bergamini et al. used MD simulations to assess the thickness of a hexapeptide monolayer on a Au(111) surface: the peptides were placed in solution and the self-assembly process was simulated by forcing the anchoring of the cysteine's sulfur atom *via* an increasing harmonic restraint on the gold-sulfur distance.[102]

On a different note, Hamad-Schifferli's group highlighted the importance of measuring both the structure and the function of a protein, after labelling it with a NP.[103] To investigate how NP binding affects protein structure and function, they systematically labelled cytochrome c (cyt c) by cysteine, mutating the surface residues in different positions.[104] Thus, a negatively charged GNP of 1.5 nm diameter, capped with bis(*p*-sulfonatophenyl) phenylphosphine ligand, was covalently bound to cyt c through a gold-sulfur bond. The labelling effects on the protein structure were measured by circular dichroism, while MD simulations gave further insights into the structural changes. Also, Stueker et al., in order to elucidate the changes in protein activity upon interaction with a NP, presented a molecular mechanics (MM) model for mercaptoundecanoic acid-capped 5 nm GNP interacting with L-lactate dehydrogenase enzyme.[105] The effect of binding was probed by MD simulations using the essential collective dynamics (ECD) method and well reflected the changes in the enzyme activity observed experimentally.

7. Conclusions and Perspectives

The ability to control the self-assembly and self-organization of small molecules at the surface of nanoparticles could pave the way to the preparation of nanomaterials with well-defined structural and (bio)physicochemical properties, which could then be envisioned to form more complex systems. Whilst getting a detailed picture remains challenging, a number of characterization techniques are available.

For instance, the optical and electronic properties of the gold core can be exploited to gather indirect evidence of ligand conjugation with UV-vis spectroscopy, whereas, upon ligand removal, separation and mass spectrometry techniques can provide more direct information about the monolayer composition. Scattering techniques can give information about the whole self-assembled monolayer, thus tackling the questions of the nanoparticles' hydrodynamic radius, stability, size dispersion and monolayer thickness. The ligands' conformation is at the basis of these observations and attempts at assessing it involve structural biology techniques, such as NMR and IR spectroscopies; sample preparation procedures have to be carefully taken into account when interpreting the results, though.

15

However, the level of molecular details that can be obtained with direct methods of characterization is limited. Thus, using a combination of experimental and theoretical approaches can provide a compelling description of the structure and organization of the monolayer. Nevertheless, advances in both areas of research are critical to work toward the rational design of nanoparticles with precise structural and (bio)physicochemical properties.

Author Information

Corresponding Author
rapha@liverpool.ac.uk
@raphavisses | Twitter
Notes
The authors declare no competing financial interest.

Acknowledgements

References

(1) Faraday, M. (1857) AuNP117-The Bakerian Lecture: Experimental Relations of Gold (and Other Metals) to Light. *Philos. Trans. R. Soc. London 147*, 145–181.

(2) Edwards, P. P., and Thomas, J. M. (2007) Gold in a Metallic Divided State—From Faraday to Present-Day Nanoscience. *Angew. Chemie Int. Ed. 46*, 5480–5486.

(3) Link, S., and El-Sayed, M. A. (2003) Optical Properties and Ultrafast Dynamics of Metallic Nanoparticles. *Annu. Rev. Phys. Chem. 54*, 331–366.

(4) Turkevich, J., Stevenson, P. C., and Hillier, J. (1951) A study of the nucleation and growth processes in the synthesis of colloidal gold. *Discuss. Faraday Soc.* 55.

(5) Brust, M., Walker, M., Bethell, D., Schiffrin, D. J., and Whyman, R. (1994) Synthesis of thiol-derivatised gold nanoparticles in a two-phase Liquid-Liquid system. *J. Chem. Soc. Chem. Commun.* 801.

(6) Häkkinen, H. (2012) The gold-sulfur interface at the nanoscale. *Nat. Chem. 4*, 443–55.

(7) Love, J. C., Estroff, L. A., Kriebel, J. K., Nuzzo, R. G., and Whitesides, G. M. (2005) Self-assembled monolayers of thiolates on metals as a form of nanotechnology. *Chem. Rev. 105*, 1103–69.

(8) Lévy, R., Thanh, N. T. K., Doty, R. C., Hussain, I., Nichols, R. J., Schiffrin, D. J., Brust, M., and Fernig, D. G. (2004) Rational and combinatorial design of peptide capping ligands for gold nanoparticles. *J. Am. Chem. Soc. 126*, 10076–84.

(9) Mirkin, C. a, Letsinger, R. L., Mucic, R. C., and Storhoff, J. J. (1996) A DNA-based method for rationally assembling nanoparticles into macroscopic materials. *Nature 382*, 607–609.

(10) Alivisatos, A. P., Johnsson, K. P., Peng, X., Wilson, T. E., Loweth, C. J., Bruchez, M. P., and Schultz, P. G. (1996) Organization of "nanocrystal molecules" using DNA. *Nature 382*, 609–11.

(11) Otsuka, H., Nagasaki, Y., and Kataoka, K. (2003) PEGylated nanoparticles for biological and pharmaceutical

applications. *Adv. Drug Deliv. Rev. 55*, 403–419.

(12) Duchesne, L., Gentili, D., Comes-Franchini, M., and Fernig, D. G. (2008) Robust Ligand Shells for Biological Applications of Gold Nanoparticles. *Langmuir 24*, 13572–13580.

(13) Chen, X., Qoutah, W. W., Free, P., Hobley, J., Fernig, D. G., and Paramelle, D. (2012) Features of Thiolated Ligands Promoting Resistance to Ligand Exchange in Self-Assembled Monolayers on Gold Nanoparticles. *Aust. J. Chem. 65*, 266.

(14) Free, P., Shaw, C. P., and Lévy, R. (2009) PEGylation modulates the interfacial kinetics of proteases on peptide-capped gold nanoparticles. *Chem. Commun.* 5009–11.

(15) Nieves, D. J., Azmi, N. S., Xu, R., Lévy, R., Yates, E. A., and Fernig, D. G. (2014) Monovalent maleimide functionalization of gold nanoparticles via copper-free click chemistry. *Chem. Commun. 50*, 13157–60.

(16) Sperling, R. A., Rivera Gil, P., Zhang, F., Zanella, M., and Parak, W. J. (2008) Biological applications of gold nanoparticles. *Chem. Soc. Rev. 37*, 1896–908.

(17) Daniel, M.-C., and Astruc, D. (2004) Gold Nanoparticles: Assembly, Supramolecular Chemistry, Quantum-Size-Related Properties, and Applications toward Biology, Catalysis, and Nanotechnology. *Chem. Rev. 104*, 293–346.

(18) Saha, K., Agasti, S., Kim, C., Li, X., and Rotello, V. (2012) Gold Nanoparticles in Chemical and Biological Sensing. *Chem. Rev. 112*, 2739–2779.

(19) Shaw, C. P., Fernig, D. G., and Lévy, R. (2011) Gold nanoparticles as advanced building blocks for nanoscale self-assembled systems. *J. Mater. Chem. 21*, 12181.

(20) Boles, M. A., Engel, M., and Talapin, D. V. (2016) Self-Assembly of Colloidal Nanocrystals: From Intricate Structures to Functional Materials. *Chem. Rev.*

(21) Sapsford, K. E., Tyner, K. M., Dair, B. J., Deschamps, J. R., and Medintz, I. L. (2011) Analyzing nanomaterial bioconjugates: A review of current and emerging purification and characterization techniques. *Anal. Chem. 83*, 4453–4488.

(22) Hostetler, M. J., Templeton, A. C., and Murray, R. W. (1999) Dynamics of place-exchange reactions on monolayer-protected gold cluster molecules. *Langmuir 15*, 3782–3789.

(23) Ghosh, S. K., and Pal, T. (2007) Interparticle coupling effect on the surface plasmon resonance of gold nanoparticles: from theory to applications. *Chem. Rev. 107*, 4797–862.

(24) Mie, G. (1908) Beiträge zur Optik Trüber Medien, Speziell Kolloidaler Metallösungen. *Ann. Phys. 330*, 377–445.

(25) Enustun, B. V., and Turkevich, J. (1963) Coagulation of Colloidal Gold. *J. Am. Chem. Soc. 85*, 3317–3328.

(26) Weisbecker, C. S., Merritt, M. V., and Whitesides, G. M. (1996) Molecular Self-Assembly of Aliphatic Thiols on Gold Colloids. *Langmuir 12*, 3763–3772.

(27) Schulz, F., Vossmeyer, T., Bastús, N. G., and Weller, H. (2013) Effect of the Spacer Structure on the Stability of Gold Nanoparticles Functionalized with Monodentate Thiolated Poly(ethylene glycol) Ligands. *Langmuir 29*, 9897–9908.

(28) Krpetić, Ž., Davidson, A. M., Volk, M., Lévy, R., Brust, M., and Cooper, D. L. (2013) High-resolution sizing of monolayer-protected gold clusters by differential centrifugal sedimentation. *ACS Nano 7*, 8881–90.

(29) Bhattacharjee, S. (2016) DLS and zeta potential – What they are and what they are not? *J. Control. Release 235*, 337–351.

(30) Gomes, I., Santos, N. C., Oliveira, L. M. A., Quintas, A., Eaton, P., Pereira, E., and Franco, R. (2008) Probing Surface Properties of Cytochrome *c* at Au Bionanoconjugates. *J. Phys. Chem. C 112*, 16340–16347.

(31) Comenge, J., Sotelo, C., Romero, F., Gallego, O., Barnadas, A., Parada, T. G.-C., Domínguez, F., and Puntes, V. F. (2012) Detoxifying Antitumoral Drugs via Nanoconjugation: The Case of Gold Nanoparticles and Cisplatin. *PLoS One* (Rozhkova, E. A., Ed.) *7*, e47562.

(32) Hostetler, M. J., Wingate, J. E., Zhong, C.-J., Harris, J. E., Vachet, R. W., Clark, M. R., Londono, J. D., Green, S. J., Stokes, J. J., Wignall, G. D., et al. (1998) Alkanethiolate Gold Cluster Molecules with Core Diameters from 1.5 to 5.2 nm: Core and Monolayer Properties as a Function of Core Size. *Langmuir 14*, 17–30.

(33) Templeton, A. C., Hostetler, M. J., Kraft, C. T., and Murray, R. W. (1998) Reactivity of Monolayer-Protected Gold Cluster Molecules: Steric Effects. *J. Am. Chem. Soc. 120*, 1906–1911.

(34) Zhou, H., Li, X., Lemoff, A., Zhang, B., and Yan, B. (2010) Structural confirmation and quantification of individual ligands from the surface of multi-functionalized gold nanoparticles. *Analyst 135*, 1210.

(35) Fisher, E. A., Duffy, S. J., and Meli, M.-V. (2015) The determination of ligand shell composition of bifunctional alkanethiol-capped gold nanoparticles using GC/MS/MS. *RSC Adv. 5*, 33289–33293.

(36) Hinterwirth, H., Kappel, S., Waitz, T., Prohaska, T., Lindner, W., and Lämmerhofer, M. (2013) Quantifying Thiol Ligand Density of Self-Assembled Monolayers on Gold Nanoparticles by Inductively Coupled Plasma–Mass Spectrometry. *ACS Nano 7*, 1129–1136.

(37) Scheffer, A., Engelhard, C., Sperling, M., and Buscher, W. (2008) ICP-MS as a new tool for the determination of gold nanoparticles in bioanalytical applications. *Anal. Bioanal. Chem. 390*, 249–252.

(38) Demers, L. M., Mirkin, C. A., Mucic, R. C., Reynolds, R. A., Letsinger, R. L., Elghanian, R., and Viswanadham, G. (2000) A Fluorescence-Based Method for Determining the Surface Coverage and Hybridization Efficiency of Thiol-Capped Oligonucleotides Bound to Gold Thin Films and Nanoparticles. *Anal. Chem. 72*, 5535–5541.

(39) Yan, B., Zhu, Z. J., Miranda, O. R., Chompoosor, A., Rotello, V. M., and Vachet, R. W. (2010) Laser desorption/ionization mass spectrometry analysis of monolayer-protected gold nanoparticles. *Anal. Bioanal. Chem. 396*, 1025–1035.

(40) Maus, L., Spatz, J. P., and Fiammengo, R. (2009) Quantification and Reactivity of Functional Groups in the Ligand Shell of PEGylated Gold Nanoparticles via a Fluorescence-Based Assay. *Langmuir 25*, 7910–7917.

(41) Zhu, Z. J., Rotello, V. M., and Vachet, R. W. (2009) Engineered nanoparticle surfaces for improved mass spectrometric analyses. *Analyst 134*, 2183–2188.

(42) Harkness, K. M., Cliffel, D. E., and McLean, J. A. (2010) Characterization of thiolate-protected gold nanoparticles by mass spectrometry. *Analyst 135*, 868–874.

(43) Pilolli, R., Palmisano, F., and Cioffi, N. (2012) Gold nanomaterials as a new tool for bioanalytical applications of laser desorption ionization mass spectrometry. *Anal. Bioanal. Chem. 402*, 601–623.

(44) Tanaka, K., Waki, H., and Ido, Y. (1988) Protein and Polymer Analyses up to m/z 100 000 by Laser Ionization Time-of-Flight Mass Spectrometry. *Rapid Commun. mass Spectrom. 2*, 151–153.

(45) Harkness, K. M., Hixson, B. C., Fenn, L. S., Turner, B. N., Rape, A. C., Simpson, C. A., Huffman, B. J., Okoli,

T. C., McLean, J. A., and Cliffel, D. E. (2010) A Structural Mass Spectrometry Strategy for the Relative Quantitation of Ligands on Mixed Monolayer-Protected Gold Nanoparticles. *Anal. Chem. 82*, 9268–9274.

(46) Harford, C. G., Hamlin, A., and Parker, E. (1957) Electron microscopy of HeLa cells after the ingestion of colloidal gold. *J. Cell Biol. 3*, 749–756.

(47) Jürgens, L., Nichtl, A., and Werner, U. (1999) Electron density imaging of protein films on gold-particle surfaces with transmission electron microscopy. *Cytometry 37*, 87–92.

(48) Ardao, I., Comenge, J., Benaiges, M. D., Álvaro, G., and Puntes, V. F. (2012) Rational Nanoconjugation Improves Biocatalytic Performance of Enzymes: Aldol Addition Catalyzed by Immobilized Rhamnulose-1-Phosphate Aldolase. *Langmuir 28*, 6461–6467.

(49) Zheng, T., Bott, S., and Huo, Q. (2016) Techniques for Accurate Sizing of Gold Nanoparticles Using Dynamic Light Scattering with Particular Application to Chemical and Biological Sensing Based on Aggregate Formation. *ACS Appl. Mater. Interfaces 8*, 21585–21594.

(50) Walkey, C. D., Olsen, J. B., Guo, H., Emili, A., and Chan, W. C. W. (2012) Nanoparticle Size and Surface Chemistry Determine Serum Protein Adsorption and Macrophage Uptake. *J. Am. Chem. Soc. 134*, 2139–2147.

(51) Belsey, N. A., Shard, A. G., and Minelli, C. (2015) Analysis of protein coatings on gold nanoparticles by XPS and liquid-based particle sizing techniques. *Biointerphases 10*, 19012.

(52) Torelli, M. D., Putans, R. A., Tan, Y., Lohse, S. E., Murphy, C. J., and Hamers, R. J. (2015) Quantitative Determination of Ligand Densities on Nanomaterials by X-ray Photoelectron Spectroscopy. *ACS Appl. Mater. Interfaces 7*, 1720–1725.

(53) Falabella, J. B., Cho, T. J., Ripple, D. C., Hackley, V. A., and Tarlov, M. J. (2010) Characterization of gold nanoparticles modified with single-stranded DNA using analytical ultracentrifugation and dynamic light scattering. *Langmuir 26*, 12740–7.

(54) Jadzinsky, P. D., Calero, G., Ackerson, C. J., Bushnell, D. A., and Kornberg, R. D. (2007) Structure of a thiol monolayer-protected gold nanoparticle at 1.1 A resolution. *Science 318*, 430–3.

(55) Azubel, M., Koivisto, J., Malola, S., Bushnell, D., Hura, G. L., Koh, A. L., Tsunoyama, H., Tsukuda, T., Pettersson, M., Hakkinen, H., et al. (2014) Electron microscopy of gold nanoparticles at atomic resolution. *Science (80-.). 345*, 909–912.

(56) Comenge, J., and Puntes, V. F. (2015) The Role of PEG Conformation in Mixed Layers: From Protein Corona Substrate to Steric Stabilization Avoiding Protein Adsorption. *Sci. Res.* 1–10.

(57) Tagliazucchi, M., Blaber, M. G., Schatz, G. C., Weiss, E. A., and Szleifer, I. (2012) Optical Properties of Responsive Hybrid Au@Polymer Nanoparticles. *ACS Nano 6*, 8397–8406.

(58) Xia, X., Yang, M., Wang, Y., Zheng, Y., Li, Q., Chen, J., and Xia, Y. (2012) Quantifying the Coverage Density of Poly(ethylene glycol) Chains on the Surface of Gold Nanostructures. *ACS Nano 6*, 512–522.

(59) Mandal, H. S., and Kraatz, H.-B. (2007) Effect of the surface curvature on the secondary structure of peptides adsorbed on nanoparticles. *J. Am. Chem. Soc. 129*, 6356–7.

(60) Templeton, A. C., Wuelfing, W. P., and Murray, R. W. (2000) Monolayer-Protected Cluster Molecules Characterization of MPCs. *Accounts Chem. 33*, 27–36.

(61) Fabris, L., Antonello, S., Armelao, L., Donkers, R. L., Polo, F., Toniolo, C., and Maran, F. (2006) Gold nanoclusters protected by conformationally constrained peptides. *J. Am. Chem. Soc. 128*, 326–36.

(62) Shaw, C. P., Middleton, D. A., Volk, M., and Lévy, R. (2012) Amyloid-derived peptide forms self-assembled monolayers on gold nanoparticle with a curvature-dependent β-sheet structure. *ACS Nano 6*, 1416–26.

(63) Rio-Echevarria, I. M., Tavano, R., Causin, V., Papini, E., Mancin, F., and Moretto, A. (2011) Water-soluble peptide-coated nanoparticles: control of the helix structure and enhanced differential binding to immune cells. *J. Am. Chem. Soc. 133*, 8–11.

(64) Folkers, J. P., Laibinis, P. E., and Whitesides, G. M. (1992) Self-assembled monolayers of alkanethiols on gold: comparisons of monolayers containing mixtures of short- and long-chain constituents with methyl and hydroxymethyl terminal groups. *Langmuir 8*, 1330–1341.

(65) Stranick, S. J., Parikh, A. N., Tao, Y.-T., Allara, D. L., and Weiss, P. S. (1994) Phase Separation of Mixed-Composition Self-Assembled Monolayers into Nanometer Scale Molecular Domains. *J. Phys. Chem. 98*, 7636–7646.

(66) Tamada, K., Hara, M., Sasabe, H., and Knoll, W. (1997) Surface Phase Behavior of n-Alkanethiol Self-Assembled Monolayers Adsorbed on Au(111): An Atomic Force Microscope Study. *Langmuir 13*, 1558–1566.

(67) Duchesne, L., Wells, G., Fernig, D. G., Harris, S. A., and Lévy, R. (2008) Supramolecular domains in mixed peptide self-assembled monolayers on gold nanoparticles. *Chembiochem 9*, 2127–34.

(68) Gentilini, C., Franchi, P., Mileo, E., Polizzi, S., Lucarini, M., and Pasquato, L. (2009) Formation of Patches on 3D SAMs Driven by Thiols with Immiscible Chains Observed by ESR Spectroscopy. *Angew. Chemie Int. Ed. 48*, 3060–3064.

(69) Harkness, K. M., Balinski, A., McLean, J. A., and Cliffel, D. E. (2011) Nanoscale Phase Segregation of Mixed Thiolates on Gold Nanoparticles. *Angew. Chemie-International Ed. 50*, 10554–10559.

(70) Jackson, A. M., Myerson, J. W., and Stellacci, F. (2004) Spontaneous assembly of subnanometre-ordered domains in the ligand shell of monolayer-protected nanoparticles. *Nat. Mater. 3*, 330–336.

(71) Cesbron, Y., Shaw, C. P., Birchall, J. P., Free, P., and Lévy, R. (2012) Stripy Nanoparticles Revisited. *Small 8*, 3714–3719.

(72) Stirling, J., Lekkas, I., Sweetman, A., Djuranovic, P., Guo, Q., Pauw, B., Granwehr, J., Lévy, R., and Moriarty, P. (2014) Critical Assessment of the Evidence for Striped Nanoparticles. *PLoS One* (Shankar, S. S., Ed.) *9*, e108482.

(73) Yu, M., and Stellacci, F. (2012) Response to "Stripy Nanoparticles Revisited." *Small 8*, 3720–3726.

(74) Ong, Q. K., and Stellacci, F. (2015) Response to "Critical Assessment of the Evidence for Striped Nanoparticles." *PLoS One* (Sangaru, S. S., Ed.) *10*, e0135594.

(75) Zaupa, G., Mora, C., Bonomi, R., Prins, L. J., and Scrimin, P. (2011) Catalytic self-assembled monolayers on Au nanoparticles: The source of catalysis of a transphosphorylation reaction. *Chem. - A Eur. J. 17*, 4879–4889.

(76) Bonomi, R., Cazzolaro, A., and Prins, L. J. (2011) Assessment of the morphology of mixed SAMs on Au nanoparticles using a fluorescent probe. *Chem. Commun. 47*, 445–447.

(77) Kohlmann, O., Steinmetz, W. E., Mao, X.-A., Wuelfing, W. P., Templeton, A. C., Murray, R. W., and Johnson, C. S. (2001) NMR Diffusion, Relaxation, and Spectroscopic Studies of Water Soluble, Monolayer-Protected Gold Nanoclusters †. *J. Phys. Chem. B 105*, 8801–8809.

(78) Pradhan, S., Brown, L. E., Konopelski, J. P., and Chen, S. (2009) Janus nanoparticles: reaction dynamics and NOESY characterization. *J. Nanoparticle Res. 11*, 1895–1903.

(79) Liu, X., Yu, M., Kim, H., Mameli, M., Stellacci, F., Pengo, P., Polizzi, S., Pasquato, L., Scrimin, P., Daniel, M.-C., et al. (2012) Determination of monolayer-protected gold nanoparticle ligand–shell morphology using NMR. *Nat. Commun. 3*, 1182.

(80) De Gennes, P. G. (1992) Soft matter. *Rev. Mod. Phys. 64*, 645–648.

(81) Perro, A., Reculusa, S., Ravaine, S., Bourgeat-Lami, E., and Duguet, E. (2005) Design and synthesis of Janus micro- and nanoparticles. *J. Mater. Chem. 15*, 3745.

(82) Walther, A., and Müller, A. H. E. (2013) Janus Particles: Synthesis, Self-Assembly, Physical Properties, and Applications. *Chem. Rev. 113*, 5194–5261.

(83) Nørgaard, K., Weygand, M. J., Kjaer, K., Brust, M., and Bjørnholm, T. (2004) Adaptive chemistry of bifunctional gold nanoparticles at the air/water interface. A synchrotron X-ray study of giant amphiphiles. *Faraday Discuss. 125*, 221–233.

(84) Andala, D. M., Shin, S. H. R., Lee, H.-Y., and Bishop, K. J. M. (2012) Templated Synthesis of Amphiphilic Nanoparticles at the Liquid–Liquid Interface. *ACS Nano 6*, 1044–1050.

(85) Charchar, P., Christofferson, A. J., Todorova, N., and Yarovsky, I. (2016) Understanding and Designing the Gold-Bio Interface: Insights from Simulations. *Small 12*, 2395–2418.

(86) Hautman, J., and Klein, M. L. (1989) Simulation of a monolayer of alkyl thiol chains. *J. Chem. Phys. 91*, 4994.

(87) Tupper, K. J., and Brenner, D. W. (1994) Molecular dynamics simulations of friction in self-assembled monolayers. *Thin Solid Films 253*, 185–189.

(88) Mahaffy, R., Bhatia, R., and Garrison, B. J. (1997) Diffusion of a Butanethiolate Molecule on a Au{111} Surface. *J. Phys. Chem. B 101*, 771–773.

(89) Gerdy, J. J., and Goodard, W. A. (1996) Atomistic Structure for Self-Assembled Monolayers of Alkanethiols on Au(111) Surfaces. *J. Am. Chem. Soc. 118*, 3233–3236.

(90) Ghorai, P. K., and Glotzer, S. C. (2007) Molecular Dynamics Simulation Study of Self-Assembled Monolayers of Alkanethiol Surfactants on Spherical Gold Nanoparticles. *J. Phys. Chem. C 111*, 15857–15862.

(91) Singh, C., Ghorai, P. K., Horsch, M. A., Jackson, A. M., Larson, R. G., Stellacci, F., and Glotzer, S. C. (2007) Entropy-Mediated Patterning of Surfactant-Coated Nanoparticles and Surfaces. *Phys. Rev. Lett. 99*, 226106.

(92) Ghorai, P. K., and Glotzer, S. C. (2010) Atomistic Simulation Study of Striped Phase Separation in Mixed-Ligand Self-Assembled Monolayer Coated Nanoparticles. *J. Phys. Chem. C 114*, 19182–19187.

(93) Velachi, V., Bhandary, D., Singh, J. K., and Cordeiro, M. N. D. S. (2015) Structure of Mixed Self-Assembled Monolayers on Gold Nanoparticles at Three Different Arrangements. *J. Phys. Chem. C 119*, 3199–3209.

(94) Van Lehn, R. C., and Alexander-Katz, A. (2013) Structure of Mixed-Monolayer-Protected Nanoparticles in Aqueous Salt Solution from Atomistic Molecular Dynamics Simulations. *J. Phys. Chem. C 117*, 20104–20115.

(95) Fetisov, E. O., and Siepmann, J. I. (2016) Structure and Phase Behavior of Mixed Self-Assembled Alkanethiolate Monolayers on Gold Nanoparticles: A Monte Carlo Study. *J. Phys. Chem. B 120*, 1972–1978.

(96) Gkeka, P., Sarkisov, L., and Angelikopoulos, P. (2013) Homogeneous Hydrophobic–Hydrophilic Surface Patterns Enhance Permeation of Nanoparticles through Lipid Membranes. *J. Phys. Chem. Lett. 4*, 1907–1912.

(97) Iori, F., Di Felice, R., Molinari, E., and Corni, S. (2009) GolP: an atomistic force-field to describe the

interaction of proteins with Au(111) surfaces in water. *J. Comput. Chem. 30*, 1465–76.

(98) Wright, L. B., Rodger, P. M., Corni, S., and Walsh, T. R. (2013) GolP-CHARMM: First-Principles Based Force Fields for the Interaction of Proteins with Au(111) and Au(100). *J. Chem. Theory Comput. 9*, 1616–1630.

(99) Todorova, N., Chiappini, C., Mager, M., Simona, B., Patel, I. I., Stevens, M. M., and Yarovsky, I. (2014) Surface presentation of functional peptides in solution determines cell internalization efficiency of TAT conjugated nanoparticles. *Nano Lett. 14*, 5229–37.

(100) Lee, K. H., and Ytreberg, F. M. (2012) Effect of Gold Nanoparticle Conjugation on Peptide Dynamics and Structure. *Entropy 14*, 630–641.

(101) Colangelo, E., Chen, Q., Davidson, A. M., Paramelle, D., Sullivan, M. B., Volk, M., and Levy, R. (2016) Experimental and Computational Investigation of the Structure of Peptide Monolayers on Gold Nanoparticles. *bioRxiv*.

(102) Bergamini, L., Voliani, V., Cappello, V., Nifosì, R., and Corni, S. (2015) Non-linear optical response by functionalized gold nanospheres: identifying design principles to maximize the molecular photo-release. *Nanoscale 7*, 13345–13357.

(103) Aubin-Tam, M.-E., and Hamad-Schifferli, K. (2008) Structure and function of nanoparticle–protein conjugates. *Biomed. Mater. 3*, 34001.

(104) Aubin-Tam, M.-E., Hwang, W., and Hamad-Schifferli, K. (2009) Site-directed nanoparticle labeling of cytochrome c. *Proc. Natl. Acad. Sci. U. S. A. 106*, 4095–100.

(105) Stueker, O., Ortega, V. A., Goss, G. G., and Stepanova, M. (2014) Understanding interactions of functionalized nanoparticles with proteins: A case study on lactate dehydrogenase. *Small 10*, 2006–2021.

22
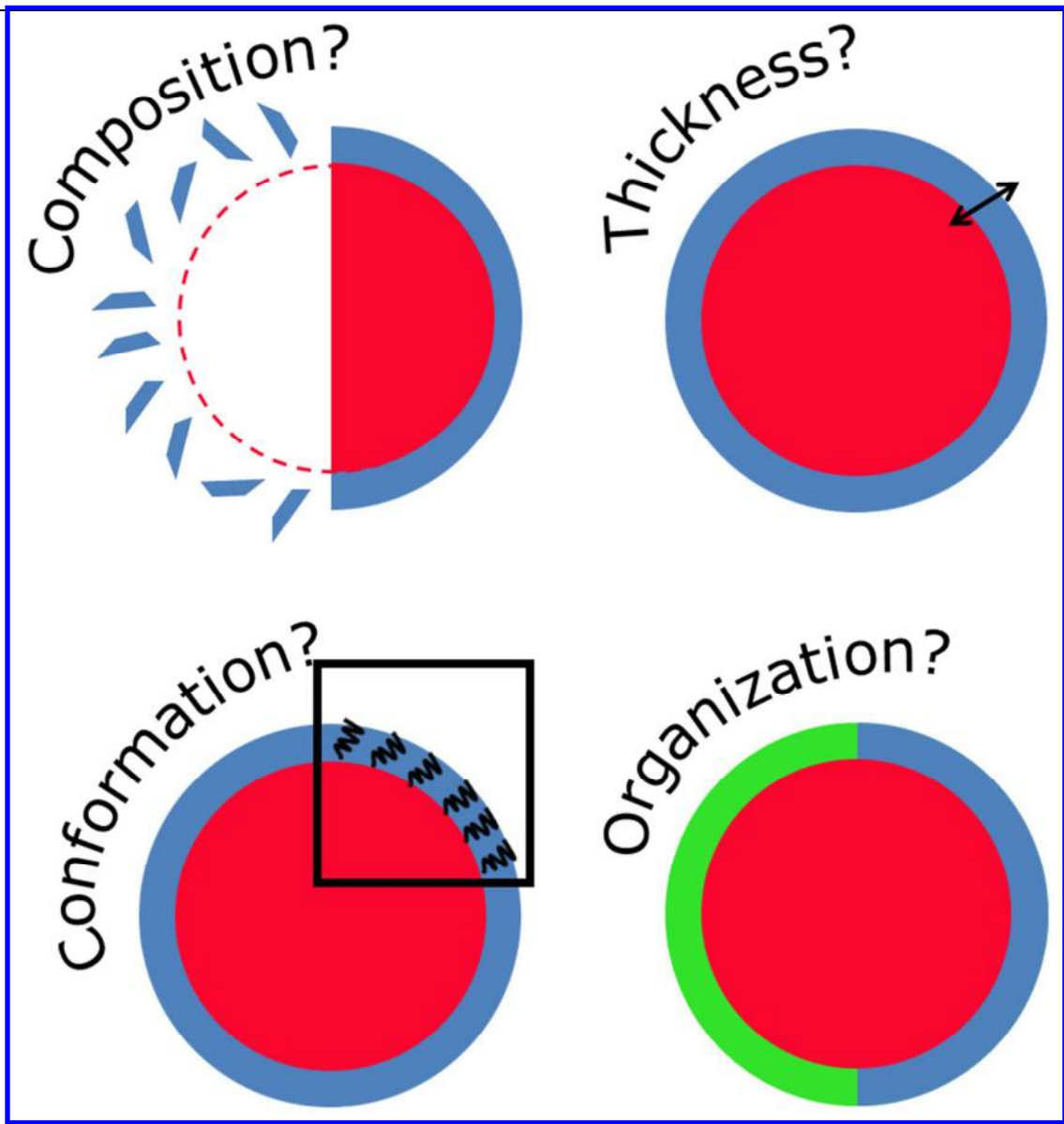
Insert Table of Contents artwork here